

ELASTICITY CHARACTERIZATION OF PIEZOELECTRIC DOMAIN BOUNDARY BY ULTRASONIC ATOMIC FORCE MICROSCOPY

T. Tsuji¹, H. Ogiso², J. Akedo², S. Saito¹, K. Fukuda¹, K. Yamanaka¹;

¹ Tohoku University, Sendai, Japan, ² AIST, Tsukuba, Japan

Abstract: Recently, in the development for piezoelectric and ferroelectric devices, the characterization method for nano-scale structure such as a ferroelectric domain and ferroelectric domain boundary (FeDB) has been important. The ultrasonic atomic force microscopy (UAFM) is expected to have the potential of elasticity characterization on the ferroelectric domain with nano-scale spatial resolution. In this work, it is demonstrated using lead zirconate titanate (PZT) ceramics. The UAFM characterized the spatial variation in the stiffness on the domain with the size from a few tens to a few hundreds of nanometers. Moreover, the high resolution imaging using a resonance frequency tracking circuit imaged the softening at the FeDB. This phenomenon may affect the piezoelectricity of PZT and the easy mobility of the FeDB under the stress and the electric field, which are important for actuator applications and high-speed writing memory applications. The potential of the UAFM is also applicable to the detection for nano-scale subsurface defects in a substrate for electronic devices.

1. Introduction: For ultrasonic transducers and precise positioning actuators, piezoelectric materials are essential. Particularly, lead zirconate titanate ($\text{Pb}(\text{Zr}_x\text{Ti}_{1-x})\text{O}_3$: PZT) is the most important material because of its high piezoelectric coefficient. Based on widely practical applications of the bulk material, PZT thin films are expected to be the actuators of micro-electro-mechanical systems [1]. Because PZT is a ferroelectric material as well as a piezoelectric material, there is a remanent polarization, which is switched by an electric field. The switching is applied to non-volatile memory devices by assigning positive and negative state of the polarization to 1 and 0, respectively (ferroelectric random access memory: FeRAM) [2].

The piezoelectricity and ferroelectricity in PZT is affected by a ferroelectric domain structure [3]. In the operation of the transducers and actuators, the domain deforms. In recording and writing in the FeRAM, a ferroelectric domain boundary (FeDB) moves. Therefore, the characterization of the domain and the FeDB probably provides useful information on effective development of PZT devices.

In PZT, the size of the ferroelectric domain is from a few tens to a few hundreds of nanometers. In general, the width of the FeDB is considered to be in the order of 1 to 10 nm [4]. It is known that an acoustic microscopy is the method that can quantitatively characterize local elasticity [5-7]. However, because the spatial resolution is limited by the wave length, it is difficult to detect the spatial variation on the structure smaller than 1 μm such as the domain. In order to overcome this limitation, we have developed the ultrasonic atomic force microscopy (UAFM) [8-14] where the elasticity can be characterized with the resolution of an atomic force microscopy (AFM) typically in the order of nm.

In this work, in order to demonstrate the potential of the UAFM in elasticity characterization on piezoelectric material, ferroelectric domain structure in PZT was investigated. It is verified that the UAFM can characterize the spatial variation in the stiffness on the domain with the size from a few tens to a few hundreds of nanometers. Moreover, it is reported that high resolution imaging by a resonance frequency tracking circuit [10] has the potential to characterize the stiffness on the FeDB, which has not been achieved by other elasticity characterization methods.

2. Measurement method and sample preparation: Figure 1 shows the principle of the UAFM [8,9]. The AFM uses soft cantilever and it is essential for obtaining a precise topography. However, the elasticity (stiffness) characterization is difficult in stiff materials such as ceramics and alloys (Fig. 1(a)) because the elastic deformation is too small to measure the spatial variation. In the UAFM, the cantilever, where the tip is in contact with the sample, is vibrated at the resonance frequency (Fig. 1(b)). The resonance vibration generates two effects; one is the inertia force of the cantilever and tip. The other is effective stiffening of the cantilever by a node

formation at higher deflection modes. Based on these effects, the UAFM can deform the stiff sample despite using the soft cantilever.

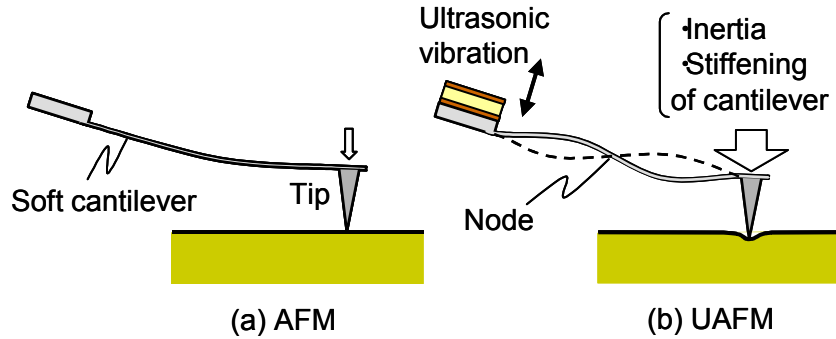


Fig. 1 Principle of UAFM. (a) AFM (b) UAFM operating at the 2nd deflection mode. Elasticity (contact stiffness) is evaluated by resonance frequency.

In the field of the AFM, the stiffness of the sample is evaluated by the contact stiffness [15] that is the spring due to the elastic contact between the tip and the sample. In the UAFM, the contact stiffness can be analyzed from the resonance frequency using the cantilever vibration theory in the UAFM [9,12]. Therefore, in order to characterize the spatial variation in stiffness, the mapping of the resonance frequency is essential.

Fig. 2 is the schematic diagram of the UAFM with a resonance frequency tracking circuit that drastically reduces the measurement time of the resonance frequency and achieves the high-spatial resolution imaging [10]. In the initial setting, the switch for the frequency feed back is opened. The resonance vibration is excited by a voltage-controlled oscillator (VCO) adjusted by an input DC bias V_0 . The phase shift of the deflection signal from the reference signal is adjusted by a phase shifter, to vanish the output DC bias V_{ERR} after the error amplifier.

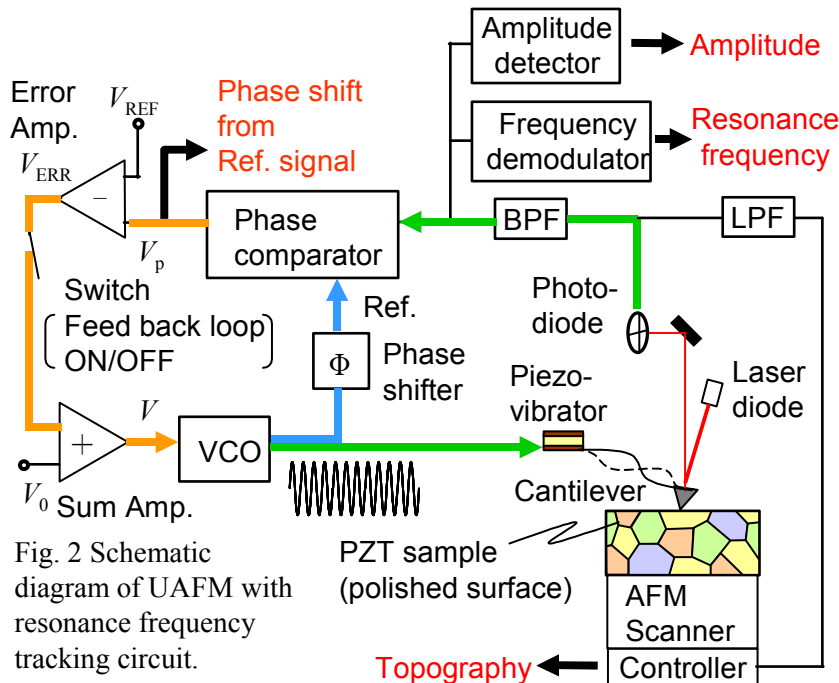


Fig. 2 Schematic diagram of UAFM with resonance frequency tracking circuit.

After the switch is closed, the raster scanning starts. If the resonance frequency is changed from the excitation frequency of the VCO output signal, non-zero V_{ERR} occurs. Because the V_{ERR} is fed back into the VCO to recover the resonance vibration, the new resonance frequency is tracked. As a result, the cantilever is always vibrated at the resonance frequency during the scanning. Using a frequency demodulator, the DC bias proportional to the resonance frequency is

continuously detected. This DC bias is calibrated to the resonance frequency by resonance spectra measured at the reference positions using a network analyzer (not shown in the figure).

In order to investigate the spatial variation on the ferroelectric domain structure, the piezoresponse force microscopy (PFM) was used [16-18]. Fig. 3 shows the principle of the PFM. PFM uses a conductive cantilever. The tip is used as a movable top electrode on the ferroelectric sample with a bottom electrode. When the tip is positively biased, out-of-plane component of the polarization induces vertical surface displacement. As a result, the deflection of the cantilever is generated (Fig. 3(a), vertical PFM). On the other hand, in-plane component (perpendicular to the cantilever axis) induces the lateral surface displacement and the torsion of the cantilever is generated (Fig. 3(b) lateral PFM). When sinusoidal signal is applied, the vertical and lateral vibration is generated to the cantilever. Because the amplitude and the phase shift from the applied signal is changed among domains due to the different direction of the polarization, the mappings of these parameters show the ferroelectric (piezoelectric) domain structure. They are measured by a conventional lock-in detection (Fig. 4).

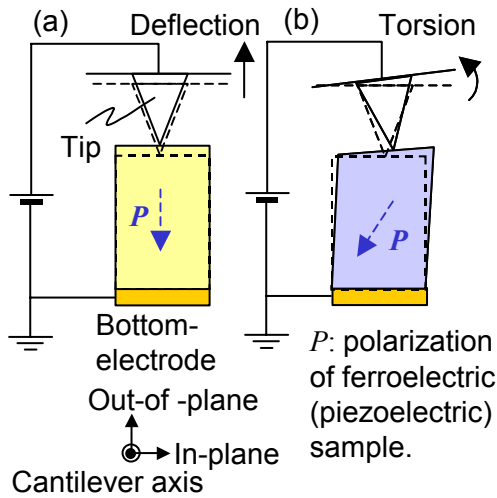


Fig. 3 Principle of PFM. (a) When tip is positively biased, (a) Purely out-of-plane component of polarization induces deflection of cantilever and (b) In-plane component induces torsion of cantilever.

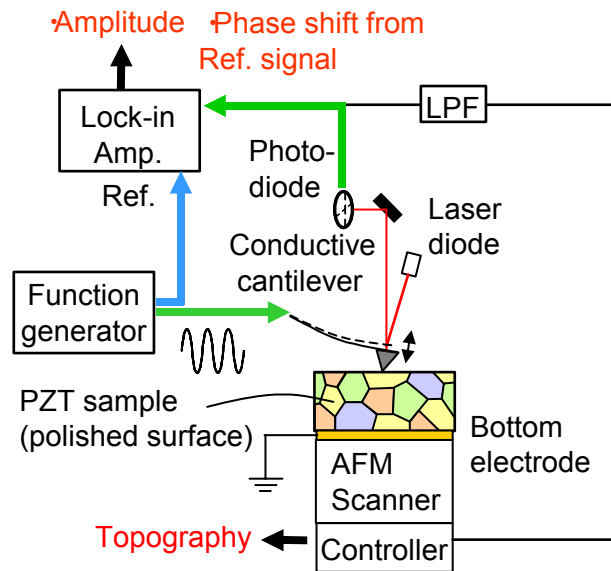


Fig. 4 Schematic diagram of PFM.

Two kinds of commercially available bulk PZT ceramics (sample 1: NEC Tokin Cooperation, N-21, sample 2: Fuji Ceramics Cooperation, C-82) were prepared for samples. Sample 1 was used for the observation of the typical domain structure. The surface was lapped by diamond slurry (3, 0.25 μm) and polished by colloidal silica slurry (Compol 80). Sample 2 was used for the observation of the FeDB. The surface was lapped by diamond slurry (1 μm) and polished by alumina paste (0.05 μm). The final thickness of both samples was approximately 0.3 mm. They were fixed on a sample holder of AFM using a silver paste. The grain size of both samples was approximately 2 μm based on an observation using an optical microscope after the surface etched by concentrated nitric acid solution. Because the ferroelectric domain structure is formed within the grain, the size of the domain is expected to be smaller than 1 μm . The experiment was performed at 23°C in ambient air with a relative humidity of approximately 50%.

3. Results and Discussions

3.1 Elasticity imaging of ferroelectric domain structure: It is known that PZT ceramics after poling show the piezoelectricity and elastic anisotropy in the direction of the remanent polarization [19]. It is strongly affected by the ferroelectric domain. In order to investigate

whether the UAFM can detect the variation in stiffness on the domain, after the domain structure was imaged by PFM, UAFM was performed.

Fig. 5 shows a result of PFM applied to sample 1. Fig. 5(a) is a topography. Although there was nano-scale groove on the grain boundary, flat surface was obtained within each grain, typically with the RMS roughness of 1 nm. Fig. 5(b) and (c) are the vertical and lateral PFM amplitude images, respectively. Broken curves represent grain boundary seen in Fig. 5(a). There was stripe structure within a grain, showing cyclic variation in converse piezoelectric displacement. It is known that the ferroelectric crystal with tetragonal structure includes 90° domain structure (Fig. 6(a) and (b)) [1,20]. On a polished surface, because cyclic variation in the direction of the polarization appears, cyclic variation in converse piezoelectricity occurs. Therefore, the stripe structure shown in Fig.5 (b) and (c) are probably 90° domain structure due to a tetragonal unit cell of PZT.

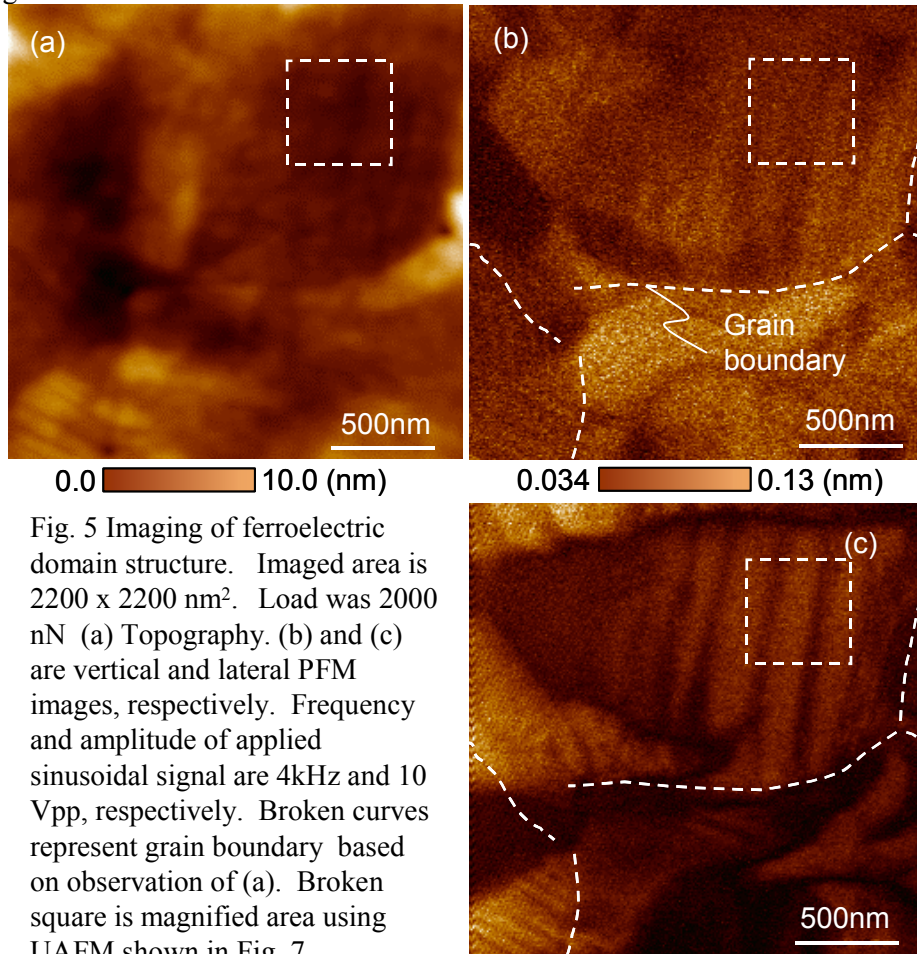


Fig. 5 Imaging of ferroelectric domain structure. Imaged area is $2200 \times 2200 \text{ nm}^2$. Load was 2000 nN (a) Topography. (b) and (c) are vertical and lateral PFM images, respectively. Frequency and amplitude of applied sinusoidal signal are 4kHz and 10 Vpp, respectively. Broken curves represent grain boundary based on observation of (a). Broken square is magnified area using UAFM shown in Fig. 7.

Here, in the unit cell of PZT with tetragonal structure, the lattice constant along c-axis (a_c) is longer than that along a-axis (a_T) (Fig. 6 (c)) [1]. Because the stiffness of the material is affected by the bond distance between atoms, the stiffness along c-axis probably becomes lower than that along a-axis. Therefore, the stripe structure is also expected to show cyclic variation in stiffness. Under this expectation, the UAFM imaging was performed within the broken square shown in Fig. 5.

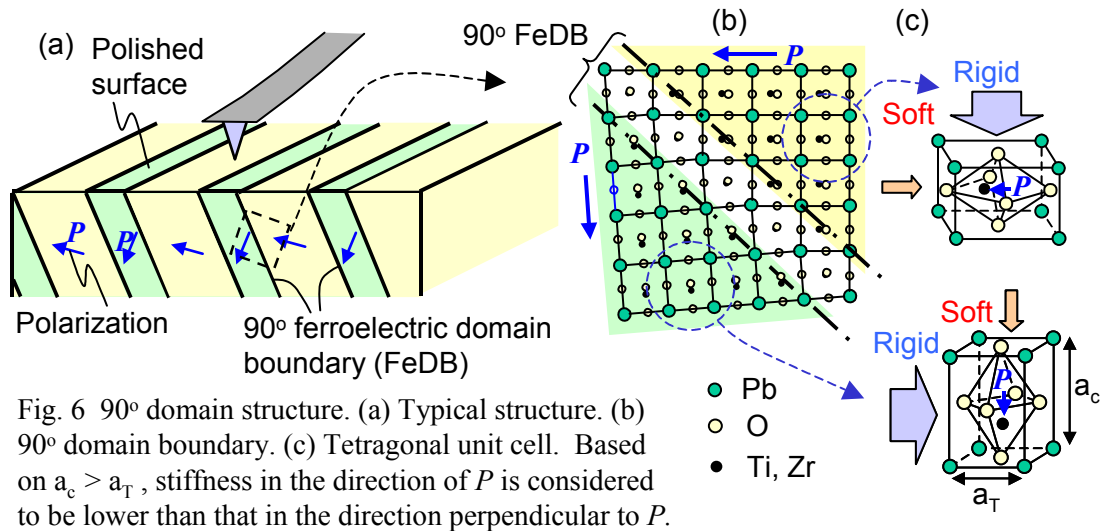
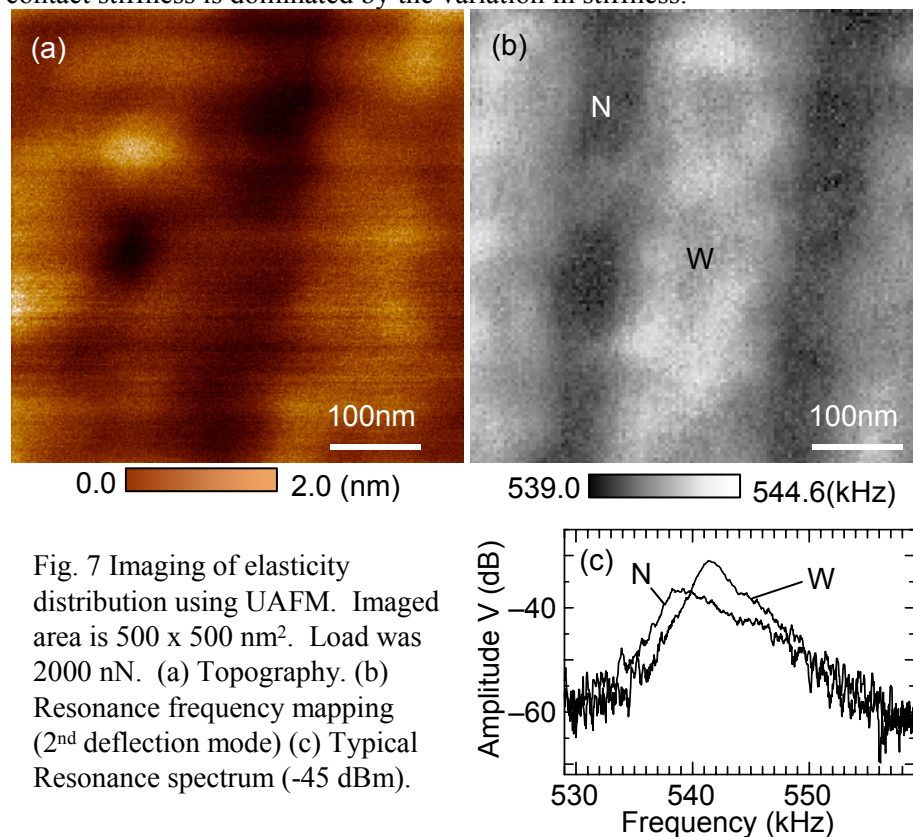


Figure 7 is a result of the UAFM. Fig. 7(a) is the topography. Fig. 7(b) is the mapping of the resonance frequency at the 2nd deflection mode. Fig. 7(c) is the resonance spectra used for the calibration for Fig. 7(b). In the UAFM image, cyclic variation in the resonance frequency was clearly observed. Based on the cantilever vibration theory in UAFM [8,9], the decrease of the resonance frequency represents the decrease of the contact stiffness. Although the contact stiffness is affected by both the stiffness of the material and the contact area [15], because the contrast shown in Fig. 7(b) is hardly affected by the topography shown in Fig. 7(a), the spatial variation in contact stiffness is dominated by the variation in stiffness.



Within the area corresponding to Fig. 7(b), we were not able to obtain the PFM images that distinguish the domains such as Fig. 5(b) and (c). However, the qualitative UAFM image using constant frequency (not shown here) showed the presence of the variation in stiffness that was related to the domain structure shown in Fig. 5(b) and (c). Therefore, Fig. 7(b) probably shows

the variation in stiffness between different domains due to the elastic anisotropy of PZT crystal. The typical width of the domain with low stiffness was approximately 50 nm and that of the domain with high stiffness was approximately 150 nm. From above discussion, it is verified that UAFM can characterize the variation in stiffness due to the ferroelectric domain structure in PZT. It was also reported in the study on the ferroelectric domain structure using atomic force acoustic microscopy [21].

3.2 Evidence for softening at ferroelectric (piezoelectric) domain boundary: During the investigation of the elasticity on PZT ceramics using the UAFM, we found interesting possibility that the stiffness on the FeDB is lower than that within the domain and evaluated the variation in stiffness on the FeDB by measuring the resonance spectra [13,14]. However, because the measurement takes a few seconds per 1 point, it is difficult to obtain detailed spatial variation in resonance frequency near the FeDB. In this report, we applied the resonance frequency tracking circuit for the rapid and detailed characterization on the FeDB.

Figure 8 shows a result measured on sample 2. Fig. 8(a) is a topography. Fig. 8(b) is a vertical PFM phase image. Bright and dark areas show the domains with the opposite direction of the polarization, respectively. The boundary between domains is considered to be the FeDB. Fig. 8(c) is the UAFM resonance frequency image at the 2nd deflection mode. Note that bright colour represents lower resonance frequency. In the bottom of the image, the image became noisy because the resonance frequency exceeded the upper limit of the dynamic range of the frequency demodulator in that setting.

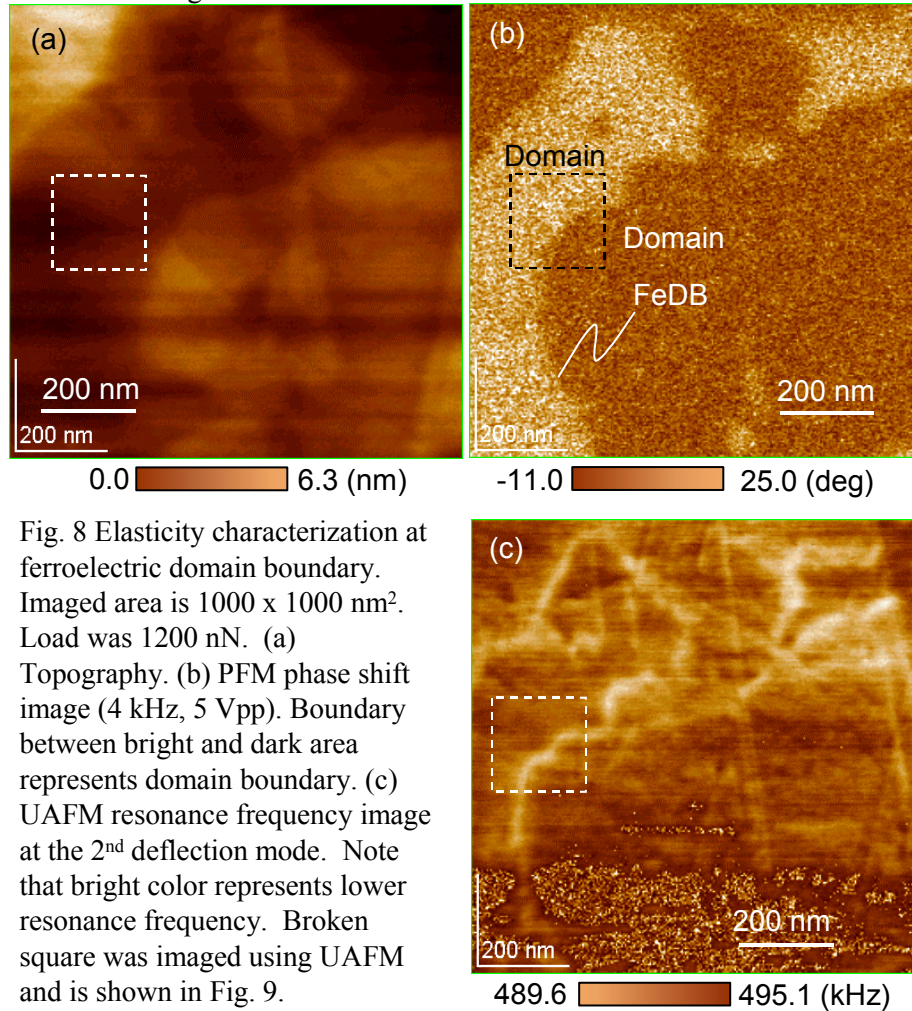


Fig. 8 Elasticity characterization at ferroelectric domain boundary. Imaged area is 1000 x 1000 nm². Load was 1200 nN. (a) Topography. (b) PFM phase shift image (4 kHz, 5 Vpp). Boundary between bright and dark area represents domain boundary. (c) UAFM resonance frequency image at the 2nd deflection mode. Note that bright color represents lower resonance frequency. Broken square was imaged using UAFM and is shown in Fig. 9.

There were string-like objects represented by the resonance frequency lower than that within the domain. Based on the comparison between Fig. 8(a), (b) and (c), it was verified that most of the

string-like objects corresponded to the FeDBs. In order to investigate the spatial variation in stiffness around the FeDB in detail, the area represented by broken square was magnified (Fig. 9).

Fig. 9(a) shows the UAFM resonance frequency image at the 2nd deflection mode and Fig. 9(b) shows the 3D view of (a). As a typical profile, the last scanning line shown in front of Fig. 9(b) is discussed. The resonance frequency became the minimum at position A during passing on the FeDB. The resonance frequency gradually decreased on the domain within the distance of 50 nm from position B to A. The distance is considered to be a characteristic length of softening by the FeDB. Because the profile crosses the FeDB approximately at 40°, the real characteristic length is approximately 32 nm. This width was much wider than that of the typical value of ferroelectric domain boundary in the range of 1 to 10 nm [4]. Because a typical contact radius of UAFM is in the order of 10 nm, it is difficult to image the FeDB itself. However, because the UAFM with resonance frequency tracking circuit rapidly provides the resonance frequency image with high lateral resolution, the spatial variation in stiffness such as the characteristic length described above can be used as an index of softening by the FeDB. The implication of softening by the FeDB is that it may affect the piezoelectricity of PZT and the easy mobility of the FeDB under the stress and the electric field.

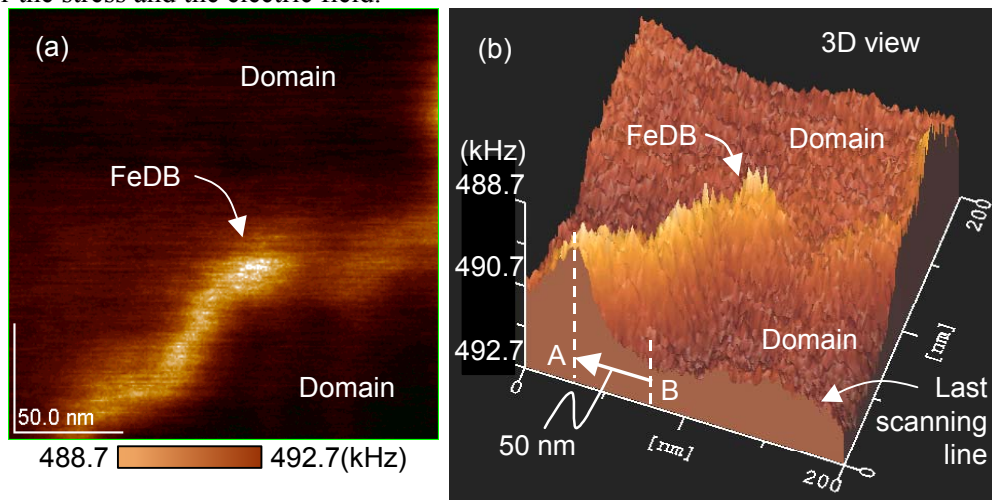


Fig. 9 Detailed observation of domain boundary. Imaged area is 200 x 200 nm². Load was 1200 nN. (a) UAFM resonance frequency image at the 2nd deflection mode. (b) 3D view of (a).

4. Conclusions: The potential of the UAFM in elasticity characterization on piezoelectric ceramics was demonstrated using the ferroelectric domain structure in commercially available PZT ceramics. The UAFM characterized the spatial variation in the stiffness on the domain with the size from a few tens to a few hundreds of nanometers. Moreover, the high resolution imaging using the resonance frequency tracking circuit characterized the stiffness of the FeDB, which has not been achieved by other elasticity characterization methods. Because the resolution of the UAFM is limited to the contact area, the direct measurement of the stiffness of the FeDB itself is difficult. However, the resonance frequency image with high lateral resolution can provide the elasticity characterization index such as the distance showing the spatial variation in stiffness. The softening at the FeDB may affect the piezoelectricity of PZT and the easy mobility of the FeDB under the stress and the electric field, which are important for not only actuator applications but also high-speed writing memory applications. The implication of this work is the high-resolution elasticity characterization method for the nano-scale structure in stiff materials such as the ferroelectric domain and the FeDB. The potential of this method is also applicable to the detection for nano-scale subsurface defects in a substrate for electronic devices.

Acknowledgement: The authors are grateful to Y. Kawakami of NEC Tokin Cooperation for useful discussion and providing piezoelectric ceramic sample. This work was supported by the fellowship of Japan Society for the Promotion of Science for Young Scientists, and by Grant in

Aid for Science Research (No. 13450017, 15656179) from the Ministry of Education, Culture, Sports, Science and Technology.

References:

1. D. Damjanovic: Rep. Prog. Phys. **61** (1998) 1267.
2. O. Auciello, J. F. Scott and R. Ramesh: Phys. Today **51** (1998) 22.
3. P. W. Rehrig, W. S. Hackenberger, S. -E. Park and T. R. Shurout: *Piezoelectric Materials in Devices*, ed. N. Setter (2002) Chap. 20, p. 433.
4. N. Setter: *Piezoelectric Materials in Devices*, ed. N. Setter (2002) Chap. 1, p. 1.
5. L. W. Kessler: J. Acoust. Soc. Am. **55** (1974) 909.
6. C. F. Quate, A. Atalar and H. K. Wickramasinghe: Proc. IEEE **67** (1979) 1092.
7. J. Kushibiki and N. Chubachi, Material characterization by line-focus-beam acoustic microscopy, IEEE Trans. Sonics and Ultrason., **SU-32** (1985) 189.
8. K. Yamanaka. and S. Nakano: Jpn. J. Appl. Phys. **35** (1996) 3787.
9. K. Yamanaka, A. Noguchi, T. Tsuji, K. Koike and T. Goto: Surf. Interface Anal. **27** (1999) 600.
10. K. Yamanaka, Y. Maruyama, T. Tsuji and K. Nakamoto: Appl. Phys. Lett. **78** (2001) 1939.
11. T. Tsuji, H. Irihama and K. Yamanaka: Jpn. J. Appl. Phys. **41** (2002) 832.
12. K. Fukuda, H. Irihama, T. Tsuji, K. Nakamoto and K. Yamanaka: Surf. Sci. **532** (2003) 1145.
13. T. Tsuji, H. Ogiso, K. Fukuda and K. Yamanaka: 30th Annual Review of Progress in Quantitative Nondestructive Evaluation **23** (2004) 1069.
14. T. Tsuji, H. Ogiso, J. Akedo, S. Saito, K. Fukuda and K. Yamanaka: Jpn. J. Appl. Phys. **43** (2004) 2907.
15. K. L. Johnson: Contact Mechanics (Cambridge University Press, Cambridge, 1985) Chap. 4, p. 84.
16. P. Guthner and Dransfeld: Appl. Phys. Lett. **61** (1992) 1137.
17. A. Gruverman, O. Auciello and H. Tokumoto: Appl. Phys. Lett. **69** (1996) 3191.
18. M. Abplanalp, L. M. Eng and P. Gunter: Appl. Phys. A **66** (1998) S231.
19. B. A. Auld: *Acoustic fields and waves in solids*, Krieger Pub. Co., (1990) Chap. 8, p. 265
20. S. Nanbu: Hyomenkagaku **17** (1996) 654 (in Japanese).
21. U. Rabe, M. Kopycinska, S. Hirsekorn, J. M. Saldana, G. A. Schneider and W. Arnold: J. Phys. D Appl. Phys. **35** (2002) 2621.